

Supramolecular Self-Assembly and Investigation of an Anthracene-linked [Pd₂L₄]⁴⁺ Cage.

Jacob Gome

Abstract

Metallosupramolecular architectures are a relatively recent class of structures which have garnered focus for a wide variety of uses. One of these uses is to bind “guests” of interest within the structure. In order to achieve this binding, cages require cavities of the correct character and shape to bind the guest molecule. This report details the synthesis of a novel ditopic ligand, L1 with pyridyl donors and an anthracene core. This ligand was subsequently used to form a [Pd₂L₄]⁴⁺ cage which was characterised by ¹H NMR spectroscopy and mass spectrometry. The host-guest properties of this cage were then investigated, demonstrating a lack of affinity for binding hydrophobic guests. Preliminary computational modelling provided a possible rationale for this lack of binding ability, suggesting that π-π interactions between anthracene linkers on the ligands resulted in a flattening of the cage structure and the lack of a well-defined cavity. This modelling was supported by ¹H NMR spectroscopy which showed an upfield shift in the anthracene protons upon the formation of the cage which can be attributed to the aforementioned π-π interactions.

I. INTRODUCTION

As the name might suggest, supramolecular self-assembly is the process during which the contents of a chemical system assemble under the influence of supramolecular interactions into a thermodynamic product. For the self-assembly process to have real use, it is desirable that the product in question is formed with high fidelity, such that allowing the reaction to proceed for a reasonable amount of time forms only a single, specific product in high yields. To achieve this, systemic conditions are designed such that the desired product is thermodynamically favourable, allowing for the high fidelity and yield.

This gives a potential advantage over more traditional synthesis techniques in constructing supramolecular architectures (Fig. 1).

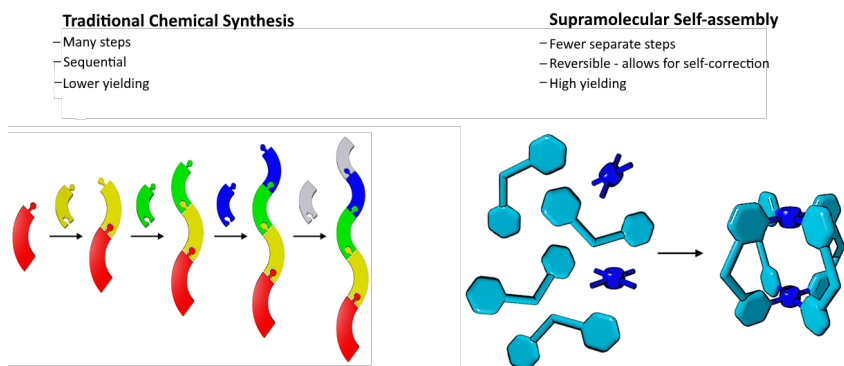


Figure 2: An image showing some of the differences between traditional chemical synthesis and supramolecular self-assembly.¹³⁵

The selectiveness of these self-assembly processes is achieved by harnessing intermolecular interactions such as hydrogen or anion bonding, π - π stacking, ion/dipole interactions and coordination bonds between a metal and a donor atom. These interactions are weaker than a typical covalent bond and are hence more reversible. This allows these

¹³⁵ These images were created in POV-Ray by Dr Dan Preston.

“bonds” to be broken and reformed continuously until the favoured (and desired) product is synthesised and thermodynamic equilibrium is reached, in essence allowing for errors in the assembly process to be corrected.

The formation of these assemblies is governed by thermodynamics, more specifically, the push-pull of entropic and enthalpic effects. Entropically, the smallest possible cyclic product is favoured, while the enthalpic contribution favours products that minimise strain within the molecule as well as maximising the number of active coordination sites. Thus, strategies are designed to preferentially form the discrete, thermodynamic product instead of polymeric, kinetic products.

This self-assembly is of particular use to synthesise discrete metallocupramolecular architectures. An early example of these within the literature is the archetypal Fujita Square[1] (Fig. 2a), containing four ethylenediamine, cis-capped palladium metal ions, linked by biphenyl units. Since then, a large variety of structures have been accessed, ranging from simple polyhedra to complex molecular knots.

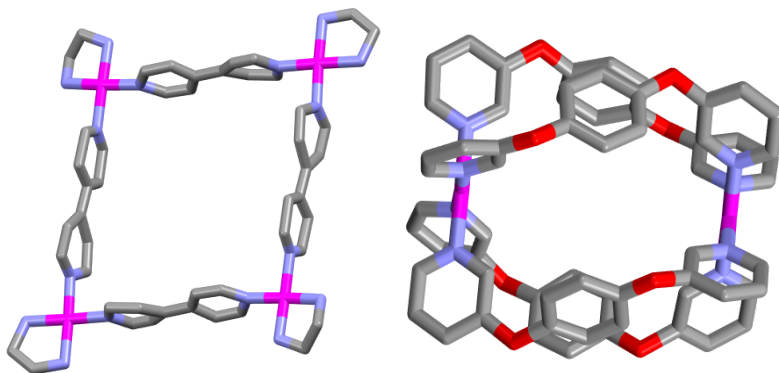


Figure 3: Depictions of X-Ray crystal structures of discrete metallocupramolecular architectures. From left to right: the first of these kinds of structures, the Fujita Square[1]; the first example of an $[M_2L_4]_{n+}$ architecture[2]. Colours: carbon grey, nitrogen blue, palladium pink, oxygen red. Hydrogen atoms and counterions excluded for clarity.

Of particular interest to this report is a subgroup of architectures, aptly named molecular cages or containers (Fig 2b.)^[2]. The molecular cage is a structure where polytopic ligands coordinate with multiple metal ions, forming an enclosed prism-like structure with a cavity, allowing the cage to encapsulate smaller molecules within it, giving the potential for host-guest chemistry.

This affinity for host-guest chemistry has been demonstrated in a variety of different applications. For instance, cages have been used to selectively sequester certain molecules such as polycyclic aromatic hydrocarbons (PAHs), a form of environmental pollutant^[3]. For this specific purpose, a self-assembling molecular container was designed by Peinador and co-workers such that it contained electron-poor aromatic arms (Fig. 3a). These aromatics can interact with the PAHs, utilising π -stacking to achieve host-guest properties that trap these pollutants, but not others, removing them from the environment. This demonstrates how cavities within such assemblies can be rationally designed to provide selectivity and specificity of host-guest interactions.

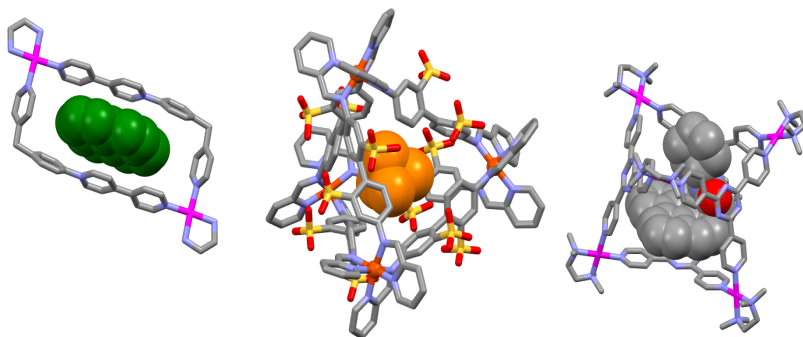


Figure 4: Depictions of X-Ray crystal structures of a variety of molecular containers. From left to right: $[\text{pyrene} \subset \text{Pd}_2(\text{en})_2(\text{L})_2]^{6+}$; $[\text{P}_4 \subset \text{Fe}_4(\text{L})_6]^{4+}$; $[\text{Adduct} \subset \text{Pd}_6(\text{en})_6(\text{L})_4]^{12+}$. Colours: carbon grey, nitrogen blue, palladium pink, oxygen red, sulphur yellow, iron orange. Hydrogen atoms and counterions excluded for clarity.

In a similar vein, molecular cages can be designed to bind otherwise unstable compounds, acting as a molecular container. White phosphorus (P_4) is renowned for being a pyrophoric compound, igniting in air and thus must be stored in water. However, white phosphorus can be made air-stable by encapsulating it within a molecular cage^[4] reported by Nitschke and co-workers (Fig. 3b). In the example described above, the cage is hypothesised to entrap the molecule within a cavity small enough so that dioxygen cannot enter the cavity to react, demonstrating the importance of cavity size in host-guest interactions.

Metallosupramolecular cages can also be used as a novel form of a molecular reaction vessel, allowing many reactions that have previously been inaccessible to be performed with relatively high yields. A $Pd(II)_6(en)_6(L)_4$ cage in D_2O was used by Fujita and co-workers to catalyse the [2+4] cycloaddition of maleic anhydride and an arene^[5] to give the endo product, a reaction that did not occur in the absence of the cage. It is hypothesised that the hydrophobicity of the substrates is the driving force for their encapsulation. Within the cavity, their spatial proximity and orientation resulted in the formation of the specific product.

A. Aims of this project

This project looks to synthesise a family of these molecular cages, in order to investigate their properties, structure and potential for host-guest chemistry. Specifically, this work seeks to synthesise ligands with pyridine donors with bis-ethynyl aryl linkers (Fig. 4). Solubilising ethylene glycol chains will also be appended. These ligands differ in the central aromatic spacer, either a phenyl or an anthracene ring. The two ligands will then be combined with palladium ions, to form $[Pd_2L_4]^{4+}$ cages, which will differ in their host-guest properties due to the different spacer groups.

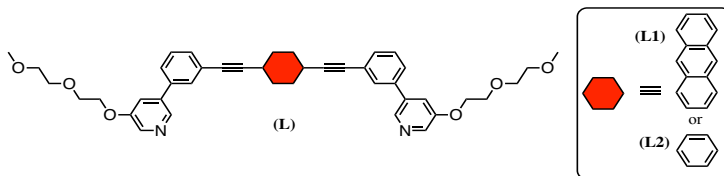


Figure 5: The ligands used in this work where the red ring can either be an anthracene ring (L1) or a phenyl ring (L2).

The host-guest properties of these cages will then be investigated, using a variety of guests. The cavity is predicted to be extremely hydrophobic for the L1 ligand, courtesy of the large aromatic surfaces within the ligand. Thus, hydrophobic guests, such as alkanes are expected to bind well within the cage. The $[\text{Pd}_2\text{L1}_4]^{4+}$ and $[\text{Pd}_2\text{L2}_4]^{4+}$ cages are expected to differ in their cavity character, including the size of the portals into the cavity, with the larger anthracene panels providing a more closed cavity.

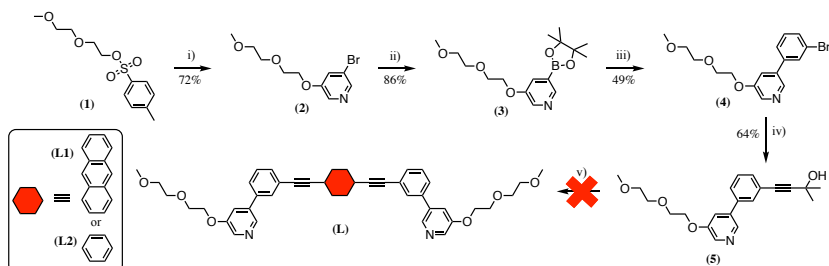
II. RESULTS AND DISCUSSION

A. Ligand Synthesis:

Initially, this work sought to synthesise a pair of ligands, L1 and L2. These ligands would differ only in the central aromatic system, displayed in red below (Scheme 1), which would consist of either a phenyl or anthracene ring. This would provide two similar cages whose host-guest properties could be investigated and compared. To this end, a synthesis plan was devised to allow for late-stage diversification, whereby the spacer group, designated by a red hexagon below could be altered at the final step to produce the two ligands (Scheme 1). Compound 2 was obtained from a Williamson ether synthesis between a tosylate ether and a pyridyl ether. 2 then underwent a Miyaura borylation to form 3 which allowed for a Suzuki coupling to afford novel compound 4. 4 was then reacted with 2-methyl-3-butyn-2-ol in a Sonogashira coupling producing 5, which forms the arm of the target

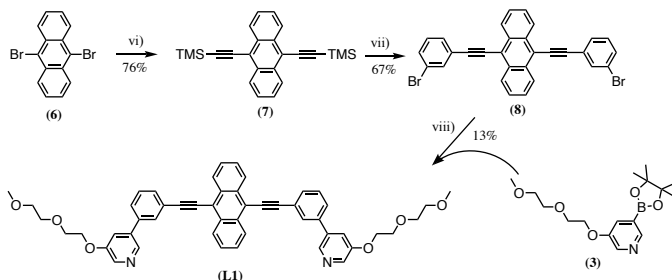
ligand. All these compounds were synthesised using well-established methods, affording the products in reasonable yields.

However, the final reaction, a deprotection followed by a double Sonogashira failed to proceed. No product was detected for L2, for L1, purification and separation from by-products in the reaction was unsuccessful.



Scheme 1: i) 5-bromopyridin-3-ol (0.67 eq.), K_2CO_3 (1 eq.), DMF, 90 °C, O/N; ii) KOAc (2.5 eq.) bis(pinacolato)diboron (1.1 eq.), $[Pd(CH_3CN)Cl_2]$ (0.05 eq.), Dppf (0.05 eq.), DMF, 90 °C, O/N; iii) Na_2CO_3 (8 eq.), 3-bromiodobenzene (2 eq.), $[Pd_2(dba)_3]$ (0.05 eq.), $[HP(t-Bu)_3]BF_4$ (0.2 eq.), DMF, 50 °C, O/N; iv) 2-methyl-3-butyn-2-ol (2 eq.), CuI (0.1 eq.), $[Pd(PPh_3)Cl_2]$ (0.05 eq.), DMF, TEA, 90 °C, O/N; v) 1. KOH (6 eq.), Toluene, 120 °C, 1 hr; 2. 1,4-diodobenzene OR 9,10-dibromoanthracene (0.48 eq.), $[Pd_2(dba)_3]$ (0.05 eq.), PPh₃ (0.2 eq.), CuI (0.1 eq.), THF/TEA (1:1), r.t., O/N

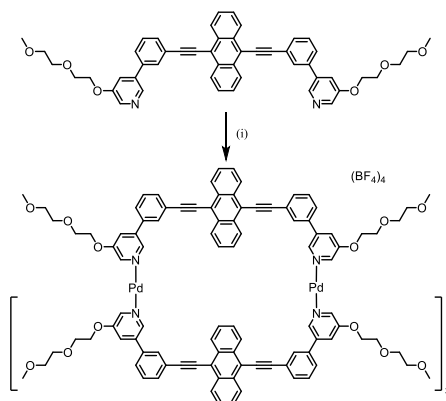
An alternate route was therefore explored, building up from the anthracene core (Scheme 2). This had the advantage of following the literature method for the double Sonogashira reaction, allowing this step to be completed first. For this method, 9,10-dibromoanthracene was initially reacted with TMS-acetylene via a Sonogashira coupling in a sealed tube to form 6. Then, 6 was deprotected *in situ*, before undergoing a Sonogashira coupling with 3-bromiodobenzene, reacting selectively with the iodo- position, affording 7. 7 was then coupled with 3 in a second Suzuki reaction, affording the target ligand L1. Due to time constraints, L2 was unable to be synthesised with this method.



Scheme 2: vi) TMS-acetylene (2.5 eq.), CuI (0.1 eq.), [Pd(PPh₃)Cl₂] (0.05 eq.), TEA, 90°C, O/N; vii) DBU (12 eq.), 3-bromoiodobenzene (2.5 eq.), CuI (0.1 eq.), [Pd(PPh₃)Cl₂] (0.05 eq.), H₂O (0.4 eq.), toluene, r.t., O/N; viii) (3) (2.5 eq.), NaCO₃ (8 eq.), [Pd₂(dba)₃] (0.05 eq.), [HP(t-Bu)₃]BF₄ (0.2 eq.), DMF, 50°C, O/N

B. Cage Formation:

To synthesise the cage, four equivalents of L1 were combined with two equivalents of [Pd₂(CH₃CN)](BF₄)₂ to afford the [Pd₂L₄](BF₄)₄ architecture (Scheme 3), in [D₆]DMSO solution. A ¹H NMR spectrum of the solution (Fig. 6) was taken. The spectrum revealed a new set of resonances that can be associated with the cage, whilst also showing the absence of any free ligand.



Scheme 3: i) [Pd(CH₃CN)₄](BF₄)₂ (2 eq.), L1 (4 eq.), [D₆]DMSO (500 μL), r.t, 15 min.

Evidence for the cage's synthesis can be found in the comparison of the spectra of the ligand and complex (Fig. 6). Certain ^1H environments in the ligand (top) experience a large change in chemical shift when combined with Pd^{2+} ions (bottom). This fits with expectations of a $[\text{Pd}_2\text{L}_4]^{4+}$ architecture having formed. Particularly noticeable are the large upfield shifts of the anthracene m and n protons. Upon the formation of the cage, the bulky aromatic panels of anthracene are expected to interact via π - π stacking, an interaction that would not be present within the free ligand solution. This π - π stacking gives a shielding effect, causing the observed shifts.

Additionally, it is interesting to note large downfield shifts of the pyridyl protons f and h. This arises from complexation of the Pd^{2+} metal ions, resulting in a withdrawal of electron density from the pyridyl ring. This in turn de-shields these protons, leading to the observed shifts.

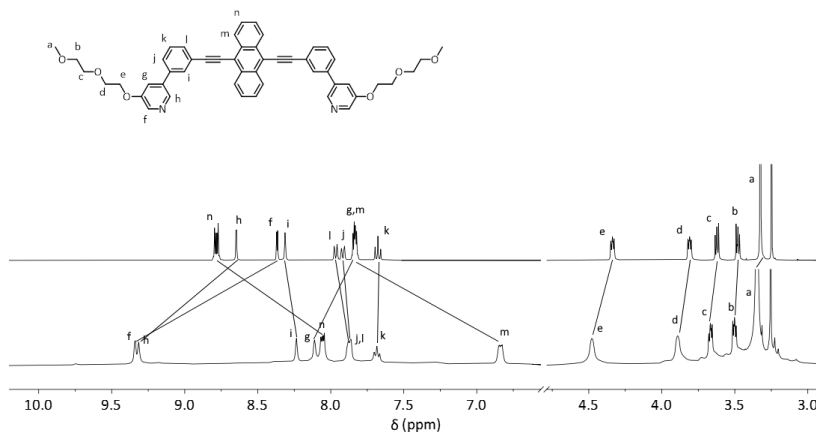


Figure 6: Partial stacked ^1H NMR spectra ($[\text{D}_6]\text{DMSO}$, 400 MHz, 298 K) of L1 (top) and the $[\text{Pd}_2(\text{L}1)_4]^{4+}$ cage (bottom).

In addition to ^1H NMR, high-resolution ESI mass spectrometry was used to confirm the presence of the cage (Fig. 7). Distinct peaks were observed for various cage/counterion combinations, for example, the peak at $m/z = 821.7776$ corresponds to a simulated peak for the

$[\text{Pd}_2\text{L}_4]^{4+}$ species. The enlarged regions shown below show the simulated (blue) and experimental (black) data for each peak with their similarity unequivocally confirming the presence of the desired $[\text{Pd}_2\text{L}_4]^{4+}$ cage.

C. Host-Guest Studies

A number of hydrophobic guests were screened by ^1H NMR spectroscopy to investigate whether they would bind within the cage. Initially, perfluorinated guests were chosen due to their extremely hydrophobic nature. These guests all showed little affinity for the DMSO solvent and thus it was hoped they would favourably bind within the cage's hydrophobic cavity. However, the ^1H NMR spectra showed no shifts in the cage peaks, indicating no binding had occurred. The screening process was then repeated with an alkyl and a phenyl tosylate salt. These guests were much more soluble in DMSO but again showed no binding within the cage.

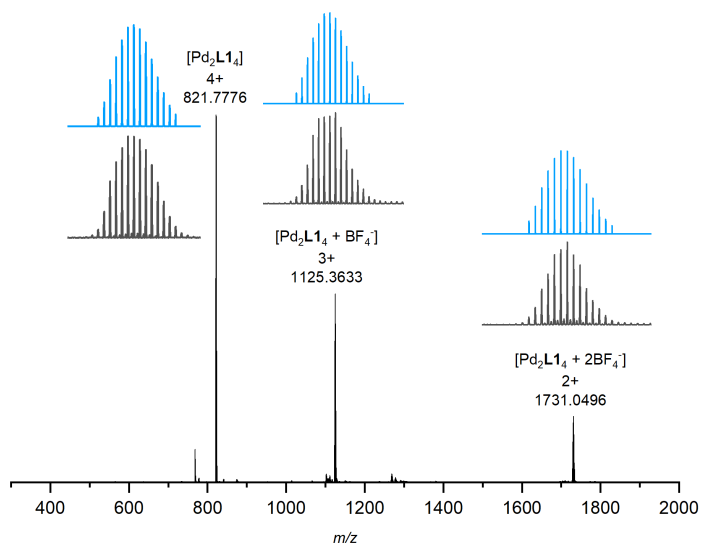


Figure 7: HR-ESI mass spectrum ($[\text{D}_6]$ DMSO/acetonitrile) of $[\text{Pd}_2\text{L}_4]^{(4-n)+}(\text{BF}_4)_n$. The enlarged regions show the simulated (blue) and experimental (black) data of each peak.

D. Computational Modelling

In an attempt to explain this lack of host-guest activity, the cage's conformation in solution, the system was modelled computationally in a preliminary fashion.¹³⁶ A short (200 ps) molecular dynamic (MD) calculation was run, with optimisation done at the GFN2-xtb level of theory using the XTB program^[6]. Standard settings were used, with a DMSO implicit solvent field at 298 K.

Inspection of the conformation of the cage (and its cavity) during the simulation indicated that the preferred structure in solution seemed to contain no well-defined cavity (Fig. 8). Instead, the adopted conformation contains strong π - π stacking interactions between two pairs of anthracene rings. This model is supported by the stacked ¹H NMR data (Fig. 6), in which the anthracene protons experience a large upfield shift. This can be attributed to the large amounts of shielding present from the aromatic stacking. These interactions flatten out the cage and appear to suggest that the cage has no clearly defined cavity.

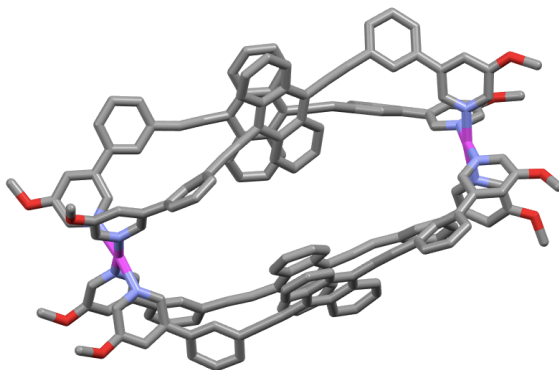


Figure 8: A representative image from the simulation of molecular dynamics. Note that the glycol ether chains were replaced with methoxy groups for computational simplicity. Colours: carbon grey, nitrogen blue, palladium pink, oxygen red. Hydrogen atoms and counterions are excluded for clarity.

¹³⁶ These computations were run by Dr Dan Preston.

III. CONCLUSIONS AND FUTURE WORK

In conclusion, a novel ligand L1 was synthesised and characterised. This ligand was used to form a [Pd2L14]⁴⁺ metallosupramolecular architecture. While this structure was initially designed as a host cavity for hydrophobic guests, screenings of a variety of these yielded no results. The lack of host-guest activity was rationalised by molecular dynamics calculations, which seem to indicate that in solution, the structure has no well-defined cavity.

Future work would seek to synthesise the phenyl analogue L2 in order to create a [Pd2L24]⁴⁺ architecture. This would allow for comparison between the two metallosupramolecular structures, particularly with regard to their host-guest activity. The L2 cage would be expected to have a better-defined cavity, due to reduced π - π stacking between the phenyl linkers. Thus, it may be more susceptible to encapsulating guest molecules.

Other linker groups could also be investigated, such as naphthyl or pyridinyl linkers. Again, these differing ligands would be expected to exhibit different host-guest properties. Additionally, heteroleptic architectures could also be investigated, allowing for a wider range of cavities to be created, potentially optimising guest-binding affinities.

IV. EXPERIMENTAL SECTION

General experimental procedure, all spectra and compound labelling are contained within the supporting information document which was submitted with this report.

(1)^[8]

2-(2-methoxyethoxy)ethyl 4-methylbenzenesulfonate^[7] (1.67 g, 6.09 mmol), 5-bromo-pyridin-3-ol (0.708 g, 40.7 mmol) and K₂CO₃ (0.842 g, 6.09 mmol) were combined in a round bottom flask. DMF was added

as a solvent (10 mL) and the mixture was heated at 90 °C overnight. DCM (~30 mL) was added, and the organic layer was washed with water (5 x 100 mL). The solvent was removed under vacuum, leaving a dark reddish-brown oil containing **(2)**. The product was then purified by column chromatography on silica (DCM to 1:5 acetone/DCM) yielding 0.778 g (69%) of pale yellow oil.

$^1\text{H NMR}$ (400 MHz, CDCl_3 , 298 K) δ : 8.32 (d, $J = 1.7$ Hz, 1H, H_h), 8.30 (d, $J = 2.5$ Hz, 1H, H_f), 7.61 (dd, $J = 2.1, 2.1$ Hz, 1H, H_g), 4.23 (m, 2H, H_e), 3.87 (m, 2H, H_d), 3.69 (m, 2H, H_c), 3.56 (m, 2H, H_b), 3.38 (s, 3H, H_a). HR ESI-MS (DCM/MeOH) $m/z = 276.0240, 278.0220$ [MH] $^+$ (calc. for $\text{C}_{10}\text{H}_{15}\text{BrNO}_3$, 276.0235, 278.0216).

(2) (0.778 g, 2.82 mmol), KOAc (0.694 g, 7.07 mmol), bis(pinacolato)diborane (0.790 g, 3.11 mmol), $[\text{Pd}(\text{CH}_3\text{CN})_2]\text{Cl}_2$ (36.7 mg, 0.014 mmol) and DPPF (78.4 mg, 0.014 mmol) were combined in a round bottom flask. DMF was added as a solvent (5 mL) and the mixture was heated at 90 °C overnight under nitrogen. DCM (~50 mL) was added, and the organic layer was washed with water (5 x 200 mL). The solvent was removed under vacuum, leaving a black sludge containing **(3)**. The product was used in subsequent steps without further purification. This was characterised by $^1\text{H NMR}$ spectroscopy and from the integration of peaks, the yield was found to be 0.819 g (86%).

$^1\text{H NMR}$ (400 MHz, CDCl_3 , 298 K) δ : 8.57 (s, 1H, H_h), 8.40 (s, 1H, H_f), 7.73 (s, 1H, H_g), 4.24 (m, 2H, H_e), 3.88 (m, 2H, H_d), 3.70 (m, 2H, H_c), 3.58 (m, 2H, H_b), 3.39 (s, 3H, H_a), 1.35 (s, 12H, H_i).

Mass spectral analysis was unsuccessful for this compound.

(3) (1.87 g, 5.78 mmol), Na_2CO_3 (4.90 g, 46.2 mmol), 1-bromo-3-iodobenzene (3.27 g, 11.6 mmol), $[\text{Pd}_2(\text{dba})_3]$ (0.264, 0.290 mmol) and $[\text{HP}(\text{t-bu})_3]\text{BF}_4$ (0.335 g, 1.16 mmol) were combined in a round bottom flask. DMF was added as a solvent (5 mL) and the mixture was heated at 50 °C overnight under nitrogen. DCM (~50 mL) was added, and the

organic layer was washed with water (5 x 150 mL). The solvent was removed under vacuum, leaving a dark brown oil containing **(4)**. The product was purified by column chromatography on silica (DCM to 1:5 acetone/DCM) yielding 1.00 g (49%).

^1H NMR (400 MHz, $[\text{D}_6]\text{DMSO}$, 298 K) δ : 8.49 (s, 1H, H_f), 8.31 (s, 1H, H_h), 7.98 (m, 1H, H_g), 7.76 (m, 1H, H_i), 7.70 (m, 1H, H_i), 7.61 (m, 1H, H_j), 7.45 (t, $J = 7.89$ Hz, H_k), 4.29 (m, 2H, H_c), 3.78 (m, 2H, H_d), 3.60 (m, 2H, H_c), 3.46 (m, 2H, H_b), 3.24 (s, 1H, H_a). ^{13}C NMR (100 MHz, $[\text{D}_6]\text{DMSO}$, 298K) δ : 154.9, 139.9, 139.3, 137.7, 134.8, 131.1, 131.0, 129.7, 126.2, 122.5, 119.0, 71.3, 69.7, 68.9, 67.7, 58.1. HR ESI-MS (DCM/MeOH) $m/z = 354.0529$ $[\text{MH}]^+$ (calc. for $\text{C}_{16}\text{H}_{19}\text{BrNO}_3$, 354.0529).

(4) (1.00 g, 2.84 mmol), 2-methyl-3-butyn-2-ol (0.480 g, 5.68 mmol), copper(I) iodide (0.0542, 0.283 mmol), $[\text{Pd}_2(\text{PPh}_3)_2\text{Cl}_2]$ (0.0997, 0.142 mmol) and triethylamine (~5 mL) were combined in a round bottom flask. DMF was added as a solvent (5 mL) and the mixture was heated at 90 °C overnight under nitrogen. EDTA NH_4/OH (0.1 M ~20 mL) was added (~25 mL), then DCM (~30 mL) was added and the mixture stirred vigorously for 30 minutes. The organic layer was washed with water (5 x 150 mL). The solvent was removed under vacuum, leaving **(5)**. The product was purified by column chromatography on silica (DCM to 1:2 acetone/DCM) yielding 0.651 g (64%).

^1H NMR (400 MHz, CDCl_3 , 298 K) δ : 8.37 (s, 1H, H_h), 8.25 (s, 1H, H_f), 7.53 (s, 1H, H_i), 7.42 (m, 1H, H_j), 7.37 (m, 1H, H_i), 7.33 (m, 1H, H_k), 7.31 (m, H_g), 4.18 (m, 2H, H_c), 3.83 (m, 2H, H_d), 3.66 (m, 2H, H_c), 3.51 (m, 2H, H_b), 3.32 (s, 3H, H_a), 1.57 (s, 6H, H_m). ^{13}C NMR (100 MHz, $[\text{D}_6]\text{DMSO}$, 298 K) δ : 155.0, 139.8, 137.4, 137.4, 135.5, 131.0, 129.6, 129.4, 127.1, 123.4, 118.9, 96.6, 80.2, 71.3, 69.7, 68.9, 67.7, 63.7, 58.1, 31.6. Mass spectral analysis was unsuccessful for this compound.

(5)^[10]

9,10-dibromoanthracene (100 mg, 0.298 mmol), TMS-acetylene (0.0731 g, 0.744 mmol), copper(I) iodide (0.00567 g, 0.0298 mmol),

[Pd₂(PPh)₃Cl₂] (0.0104 g, 0.0149 mmol) were combined in a degassed sealed tube. TEA was added as a solvent and the mixture was heated at 90 °C overnight under nitrogen. EDTA NH₄/OH (0.1 M ~20 mL) was added (~25 mL), then DCM (~30 mL) was added and the mixture stirred vigorously for 30 minutes. using DCM as an organic layer. The organic layer was washed with water (3 x 150 mL). The solvent was removed under vacuum, leaving **(7)**. The product was purified by column chromatography on silica (PE to 10% DCM in PE) yielding (0.84 mg, 76%).

¹H NMR (400 MHz, CDCl₃, 298 K) δ: 8.57 (m, 4H, H_n), 7.61 (m, 4H, H_m), 0.42 (s, 18 H, H_a). Mass spectral analysis was unsuccessful for this compound.

(6)

(84 mg, 0.23 mmol), m-bromiodobenzene (0.160 g, 0.567 mmol), DBU (0.414 g, 2.72 mmol), copper(I) iodide (0.00432 g, 0.0227 mmol), [Pd₂(PPh)₃Cl₂] (0.00795 g, 0.0114 mmol) and H₂O (0.00163, 0.0908 mmol) were combined in a round bottom flask. Toluene was added as a solvent (20 mL) and the mixture was stirred at r.t. under nitrogen. EDTA NH₄/OH (0.1 M ~20 mL) was added (~25 mL), then DCM (~30 mL) was added and the mixture stirred vigorously for 30 minutes. using DCM as an organic layer. The organic layer was washed with water (3 x 150 mL). The solvent was removed under vacuum, leaving **(8)**, a red powder. The product was purified by column chromatography on silica (DCM) yielding (0.82 mg, 67%).

¹H NMR (400 MHz, CDCl₃, 298 K) δ: 8.66 (m, 4H, H_n), 7.93 (t, *J* = 1.6 Hz, 2H, H_i), 7.71 (dm, *J* = 7.7 Hz, 2H, H_i), 7.68 (m, 4H, H_m), 7.57 (dm, *J* = 8.1 Hz, 2H, H_j), 7.34 (t, *J* = 7.9 Hz, 2H, H_k). ¹³C NMR (100 MHz, CDCl₃, 298K) δ: 134.3, 132.1, 131.9, 130.3, 130.0, 127.2, 127.1, 125.3, 122.4, 118.3, 100.8, 87.7. Mass spectral analysis was unsuccessful for this compound.

(7)

(82 mg, 0.15 mmol), **(2)** (0.124 g, 0.382 mmol), Na₂CO₃ (0.130 g, 1.22 mmol), [Pd₂(dba)₃] (0.0070, 0.0076 mmol) and [HP(t-bu)₃]BF₄ (0.0089 g, 0.031 mmol) were combined in a round bottom flask. DMF was added as a solvent (5 mL) and the mixture was heated at 50 °C overnight. DCM (~50 mL) was added, and the organic layer was washed with water (5 x 150 mL). The solvent was removed under vacuum. The product was purified by column chromatography on silica (DCM to 2:1 acetone/DCM) yielding a mixture of **(L1)** and **(3)**. Some of this mixture was suspended in methanol and centrifuged to give 6 mg (5%) of an orange powder (**L1**). Note that not all of the mixture was separated by centrifuge, if this had occurred, the actual yield would be 10-15 mg (8-13%).

¹H NMR (400 MHz, [D₆]DMSO, 298 K) δ: 8.78 (m, 4H, H_n), 8.64 (d, *J* = 1.8 Hz, 2H, H_h), 8.36 (d, *J* = 2.7 Hz, 2H, H_f), 8.31 (t, *J* = 1.5 Hz, 2H, H_i), 7.97 (dm, *J* = 7.9 Hz, 2H, H_l), 7.91 (dm, *J* = 7.9 Hz, 2H, H_j), 7.85 (m, 2H, H_g), 7.83 (m, 4H, H_m), 7.68 (m, 2H, H_k), 4.34 (m, 4H, H_c), 3.81 (m, 4H, H_d), 3.62 (m, 4H, H_c), 3.48 (m, 4H, H_b), 3.25 (s, 6H, H_a). ¹³C NMR (100 MHz, [D₆]DMSO, 298K) δ: 155.5, 140.6, 138.2, 137.8, 135.9, 132.0, 131.9, 130.6, 130.2, 128.6, 128.4, 127.5, 123.5, 119.8, 118.1, 103.1, 86.7, 71.8, 70.2, 69.4, 68.2, 58.6. HR ESI-MS (DCM/MeOH) *m/z* = 769.3285 [MH]⁺ (calc. for C₅₀H₄₅N₂O₆, 769.3278).

(Cage 1)

(L1) (3.00 mg, 3.90 μmol) and [Pd(CH₃CN)₄](BF₄)₂ (0.867 g, 1.95 μmol) were combined in sample vial. [D₆]DMSO was added as a solvent (500 μL) and the mixture was briefly sonicated until all of the solid had dissolved.

¹H NMR (400 MHz, [D₆]DMSO, 298 K) δ: 9.34 (d, *J* = 2.2 Hz, 8H, H_h), 9.31 (s, 8H, H_f), 8.23 (s, 8H, H_i), 8.11 (s, 8H, H_g), 8.06 (m, 16H, H_n), 7.88 (m, 8H, H_l), 7.86 (m, 8H, H_j), 7.68 (t, *J* = 7.6 Hz, 8H, H_k), 6.83 (m, 16H, H_m), 4.48 (m, 16H, H_c), 3.89 (m, 16H, H_d), 3.67 (m, 16H, H_c),

3.50 (m, 16H, H_b), 3.25 (s, 24H, H_a). HR ESI-MS ([D₆]DMSO/CH₃CN) $m/z = 821.7776$ [M]⁴⁺ (calc. for C₂₀₀H₁₇₂N₈O₂₄Pd₂, 822.00238); 1125.3633 [MBF₄]³⁺ (calc. for C₂₀₀H₁₇₃N₈O₂₄Pd₂BF₄, 1125.0330); 1731.0496 [MB₂F₈]²⁺ (calc. for C₂₀₀H₁₇₄N₈O₂₄Pd₂B₂F₈, 1730.5510).

References

- [1] M. Fujita, O. Sasaki, T. Mitsuhashi, T. Fujita, J. Yazaki, K. Yamaguchi, K. Ogura, *Chem. Comm.* **1996**, 1535-1536.
- [2] D. A. McMorran, P. J. Steel, *Angew. Chem. Int. Ed.* **1998**, *37*, 3295-3297.
- [3] V. Blanco, M. D. García, A. Terenzi, E. Pía, A. Fernández-Mato, C. Peinador, J. M. Quintela, *Chem. – Eur. J.* **2010**, *16*, 12373-12380.
- [4] P. Mal, B. Breiner, K. Rissanen, J. R. Nitschke, *Science* **2009**, *324*, 1697-1699.
- [5] M. Yoshizawa, M. Tamura, M. Fujita, *Science* **2006**, *312*, 251-254.
- [6] C. Bannwarth, S. Ehlert, S. Grimme, *J. Chem. Theory Comput.* **2019**, *15*, 1652-1671.
- [7] R. Hooper, L. J. Lyons, M. K. Mapes, D. Schumacher, D. A. Moline, R. West, *Macromolecules* **2001**, *34*, 931-936.
- [8] D. Preston, A. Fox-Charles, W. K. C. Lo, J. D. Crowley, *Chem. Comm.* **2015**, *51*, 9042-9045.
- [9] T. Y. Kim, L. Digal, M. G. Gardiner, N. T. Lucas, J. D. Crowley, *Chem. – Eur. J.* **2017**, *23*, 15089-15097.
- [10] W. Fudickar, T. Linker, *J. Am. Chem. Soc.* **2012**, *134*, 15071-15082.